American Mineralogist, Volume 78, pages 762–768, 1993

Structure refinements of beryl by single-crystal neutron and X-ray diffraction

Gilberto Artioli*
Istituto di Mineralogia, Università di Modena, I-41100 Modena, Italy
Romano Rinaldi
Dipartimento di Scienze della Terra, Università di Perugia, I-06100 Perugia, Italy
Kenny Ståhl
Division of Inorganic Chemistry, Chemical Center, University of Lund, S-22100 Lund, Sweden
Pier Francesco Zanazzi
Dipartimento di Scienze della Terra, Università di Perugia, I-06100 Perugia, Italy

Abstract

The crystal structure of beryl has been refined from single-crystal neutron and X-ray data obtained on two samples with different alkali and H_2O contents [morganite: $Al_2Be_{2.65}Li_{0.32}Si_6O_{18}\cdot(Na_{0.22}Cs_{0.08}0.54H_2O)$; aquamarine: $Al_{1.94}Fe_{0.06}Be_3Si_6O_{18}\cdot(Na_{0.02}0.28H_2O)$] in order to elucidate the ambiguities affecting the assignment of atomic species to the channel sites. Neutron data for morganite were obtained at 295 and 30 K; neutron data for aquamarine and X-ray data for both samples were obtained at room temperature. Final agreement factors for the three neutron and the two X-ray refinements are in the order [$R_{(\text{unweighted})}$] 0.034, 0.052, 0.033, 0.023, 0.022. The expected Li substitutions in the Be tetrahedral site and of Fe in the Al octahedral site were clearly confirmed by the neutron data refinements. Accurate site occupancy refinements in the 2a and 2b channel sites at 0,0,¼ and 0,0,0, obtained also through location of the H atoms, yielded two distinct configurations with Cs and H_2O at 0,0,¼ and Na at 0,0,0 in morganite, and Na and H_2O at 0,0,¼ in aquamarine (with 2b empty). The H_2O molecules attain two distinct orientations in the two samples with H-H vectors on the **ab** plane in morganite and parallel to the **c** axis in aquamarine. The H_2O orientations are in agreement with type II H_2O being present in alkali-containing beryl, and type I H_2O being present in alkali-free samples, as found by spectroscopic investigations.

Introduction

The crystal structure of beryl (ideal formula $Al_2Be_3Si_6O_{18}$, space group $P6/mcc$) consists of stacked six-membered rings of Si tetrahedra parallel to (0001), cross-linked by Be tetrahedra and Al octahedra to form a three-dimensional framework around six-membered ring channels which may host alkalis and H_2O and CO_2 molecules.

The presence of guest cations in the channels of the structure of beryl involves a complex substitutional pattern mainly affecting the Be tetrahedral and Al octahedral sites whereby the necessary charge balance takes place. Fe^{2+}, Mg, and Mn^{2+} commonly replace Al, whereas Li^+ is the most common substituent of Be. The most common alkalis entering the channels are Na and Cs, most frequently in the presence of H_2O molecules; K and Rb may also be present in lesser amounts.

The crystal chemistry of hydrous alkali-rich beryl has been the subject of several studies (Černý, 1975; Hawthorne and Černý, 1977; Černý and Simpson, 1977; Brown and Mills, 1986; Aurisicchio et al., 1988). X-ray structure refinements of such hydrous alkali-rich beryl show residual electron densities located at two crystallographically distinct sites at 0,0,¼ (site 2a) and at 0,0,0 (site 2b) (Fig. 1). Refinements of populations of these two sites using X-ray data yield two alternative interpretations, one of which assigns H_2O molecules, as well as the larger alkali ions Cs, Rb, and K, to the 2a site with the smaller Na ion in the 2b site at the center of the six-membered rings (Vorma et al., 1965; Gibbs et al., 1968; Hawthorne and Černý, 1977; Brown and Mills, 1986). The second interpretation calls for the alkalis to occupy the 2a site with H_2O molecules preferentially located at 2b (Aurisicchio et al., 1988). Either model enjoys the same degree of confidence based on the analysis of the residual electron density alone. A recent structural investigation by MAS NMR spectroscopy (Sherriff et al., 1991) left the ambiguity unresolved. The X-ray structure refinement of a newly discovered alkali-rich hydrous beryl sample from Ireland (Zanazzi, in Sanders and Doff, 1991) suggests that Na is located at site 2b and H_2O at 2a.

* Present address: Dipartimento di Scienze della Terra, Sez. Mineralogia, Università di Milano, I-20133 Milano, Italy.

0003–004X/93/0708–0762$02.00

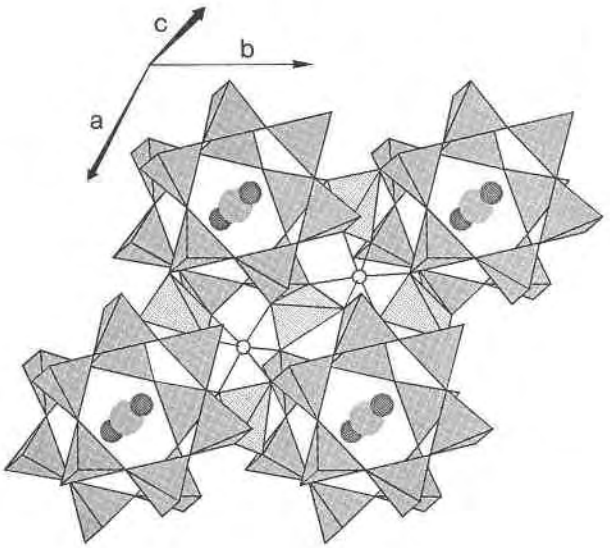

Fig. 1. The structure of beryl viewed down the **c** axis (tilted approx. 15°). Sites 2a (at 0,0,¼) and 2b (at 0,0,0) are indicated by shaded and solid circles, respectively. Lightly shaded tetrahedra represent Be (Li) polyhedra, open circles Al (Fe) octahedral sites. The hexagonal rings of Si tetrahedra (dark shade) occur at $z = 0$ and $z = ½$.

On the assumption that the negative neutron scattering length of H would help in locating the H_2O molecules and therefore in defining the distribution of the channel chemical species, we undertook a single-crystal neutron diffraction study of two natural beryl samples with different chemical compositions.

Experimental

Samples

The two beryl samples utilized in the present study were selected after screening several samples of various provenance on the basis of composition and homogeneity on a fairly large scale (10–20 mm^3).

Two square prisms with 5.3-mm^2 bases and approximately 7 mm long were cut out of the selected crystals. Each of these long prisms was then cut into two or three smaller prisms, as closely as possible approximating the shape of a cube with an easily identifiable crystallographic orientation (sample no. 1: 1.9 × 2.5 × 2.2 mm; sample no. 2: 2.5 × 2.7 × 2.2 mm), to be used in the neutron diffraction data measurements. The odd fragments resulting from the cutting were utilized for X-ray data measurements, electron probe microanalysis, thermogravimetric analysis, and infrared spectroscopy.

Sample no. 1 (pink beryl from Minas Gerais, Brazil) with a channel content of 2.0 wt% Cs_2O, 1.2 wt% Na_2O, and 1.7 wt% H_2O, pertains to the tetrahedral solid solution series (Aurisicchio et al., 1988), in which charge balance is achieved mainly by Li^+ substitution for Be^{2+} in tetrahedral sites. On account of its Cs content, this beryl sample may be classified as morganite.

Table 1. Chemical compositions of the two beryl samples

	Sample no. 1	Sample no. 2
	Oxide wt%	
SiO_2	63.34	65.41
Al_2O_3	17.80	17.94
FeO	0.05	0.77
MgO	0.01	—
Na_2O	1.15	0.09
Cs_2O	2.04	—
Li_2O	0.85*	—
BeO	11.59*	13.62*
H_2O	1.70	0.90
Total	98.53	98.73
	Atoms pfu (18 O atoms)	
Si	6.02	5.99
Al	2.00	1.94
Fe	—	0.06
Mg	—	—
Na	0.212	0.016
Cs	0.083	—
Li	0.324	—
Be	2.65	3.01
H_2O	0.53	0.28

Note: High-*Z* elements from EPMA, H_2O content from TG analysis, low-*Z* elements from neutron refinement of site populations.
* Back-calculated from neutron refinement occupancy data.

Sample no. 2 (blue beryl, variety aquamarine from Governador Valadares, Brazil) with a very low Na_2O content (0.1 wt%) pertains to the octahedral series, in which the dominant substitution is that of Fe for Al in the octahedral sites.

Chemical compositions

Wavelength dispersive (WDS) electron probe microanalysis (EPMA) of the two beryl samples was carried out with an ARL-SEMQ instrument operated at 15 kV, with a beam current (on brass) of 18 nA and a beam diameter of 6 μm. Natural silicates (albite for Na$K\alpha$, Al$K\alpha$, and Si$K\alpha$ lines; olivine for Mg$K\alpha$ and Fe$K\alpha$ lines; pollucite for the Cs$L\alpha$ line) were used as reference standards, and element concentrations were obtained on-line by a Bence-Albee data reduction procedure using Albee and Ray's (1970) correction factors. Qualitative and semiquantitative energy-dispersive analyses (EDS) carried out with an EDAX 9900 system on a Philips 515 SEM did not reveal the presence of other high-*Z* elements at a statistically significant concentration level. WDS EPMA was also carried out with a Cameca Camebax Micro instrument operated under the same conditions but with the use of the PAP analysis routine, which makes use of a $\Phi(\rho z)$ depth distribution model according to Pouchou and Pichoir (1988). The analytical results are within the statistical errors of those obtained with the ARL probe and were therefore averaged with them. The analyses, carried out on a dozen analysis points several micrometers apart on fragments of the same crystals used in the neutron diffraction experiments, gave no indication of compositional zoning exceeding the statistical uncertainty of the method. Table 1 reports the chemical compositions thus obtained for the high-*Z* elements together

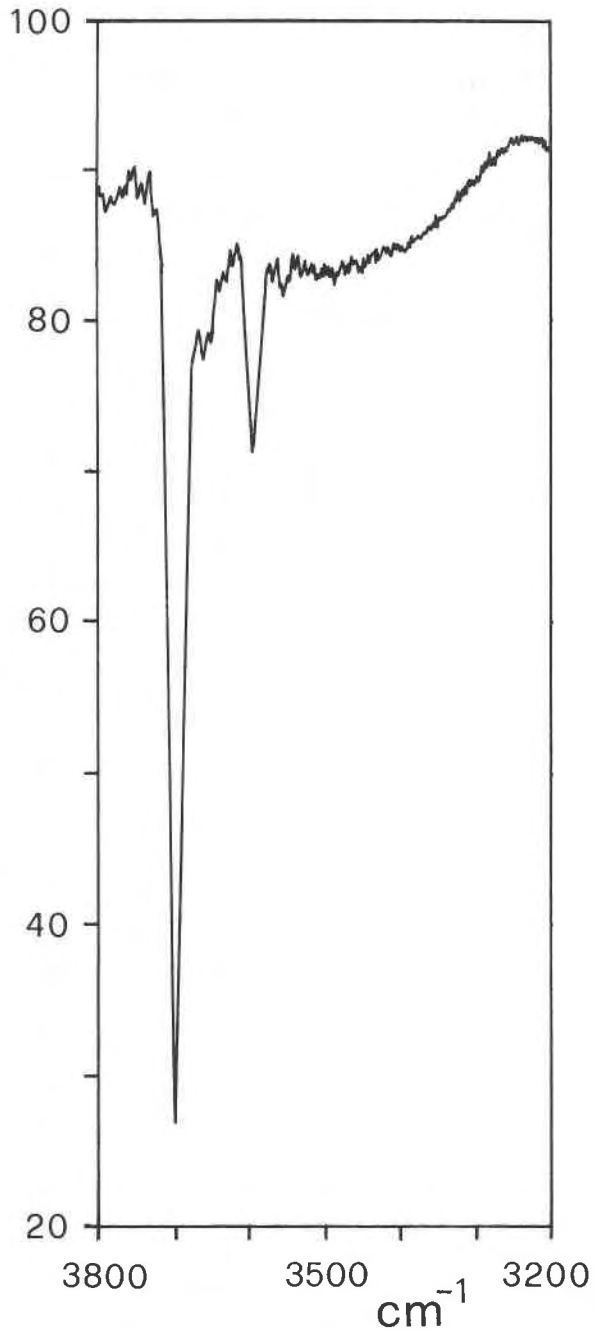

Fig. 2. Infrared spectrum (percent transmittance vs. wavenumber) of sample no. 2 showing the three peaks in the OH stretching frequency region at 3699, 3661, and 3595 cm^{-1} denoting the presence of H_2O molecules.

with estimated concentrations of the light elements (Li, Be) derived from the population refinements from the neutron data. The data thus combined provide very good overall electrostatic balances with positive charge sums of 36.01 and 36.00 (based on 18 O atoms) for crystal nos. 1 and 2, respectively.

H_2O content for sample no. 1 was determined by thermogravimetric analysis with a DuPont instrument on approximately 10 mg of powdered sample. Weight loss vs. time (20 °C/min) plotted as a gradual continuous curve from 300 to 600 °C, followed by another very gently sloping curve from 700 to 990 °C, for a total weight loss of approximately 1.70%. Weight loss on sample no. 2 was determined on a Cahn System 113 electrobalance. The powdered sample (36.529 mg) was heated to 130 °C for 30 min and then cooled to room temperature (36.516 mg). It was then heated to 1000 °C at the rate of 10 ° per minute and kept at 1000 °C for 30 min and then cooled to room temperature (36.188 mg). The difference (0.328 mg) corresponds to 0.90% H_2O, which is in good agreement with the neutron data refinement, as detailed in the discussion section. Powder from the same sample was also analyzed by infrared spectrometry using a Perkin-Elmer model 983 spectrometer in the wavenumber region between 1200 and 4000 cm^{-1}. The spectrum recorded shows three peaks in the OH stretching frequency region at 3699, 3661, and 3595 cm^{-1} (Fig. 2) and three more in the bending frequency region at 1631, 1599, and 1546 cm^{-1}. The detailed assignments of these peaks are discussed in Wickersheim and Buchanan (1959, 1965) and Wood and Nassau (1967, 1968). The small discrepancy in the H_2O content of sample no. 1 as determined from TG analysis and from neutron data structure refinement can be mainly attributed to the experimental uncertainty associated with the former, possibly due to an incomplete dehydration obtained during the TG measurement of this particular sample.

X-ray refinement

Sample no. 1. X-ray diffraction data from a small crystal fragment with dimensions 0.20 × 0.15 × 0.10 mm were obtained at room temperature with graphite monochromatized Mo$K\alpha$ radiation (λ = 0.7107 Å) on a Philips PW1100 four-circle diffractometer. Lattice parameters [a = 9.208(2), c = 9.197(2) Å] were obtained by the LAT routine of the Philips software with a least-squares procedure applied to the θ values of 35 reflections in the 12–18° range. The c/a ratio, 0.999, indicates this beryl sample belongs to the tetrahedral series (Aurisicchio et al., 1988). About 1300 reflections from the *hkl* and *khl* equivalent sectors of the reciprocal lattice were measured in the range $2 \leq \theta \leq 35°$ by the ω scan technique (scan speed 0.06°/s, scan width 2°). Three standard reflections monitored at regular intervals throughout data measurement showed no significant deviations. The intensity data were corrected for Lorentz polarization factors. An absorption correction was applied according to the semiempirical method of North et al. (1968). The values of the corrected intensities were merged to obtain a unique set of independent data (R_{eq} = 0.017); 393 reflections with $I \geq 3\sigma(I)$ were used in the least-squares refinement. The computations were carried out with the full-matrix program in the SHELX-76 crystallographic package (Sheldrick, 1976), starting from the atomic coordinates of synthetic beryl (Gibbs et al., 1968). Individual anisotropic

thermal parameters were refined for each atom. A difference Fourier map showed two residual maxima in the channel sites at 0,0,¼ (site 2a) and 0,0,0 (site 2b) corresponding to 5.28 and 1.25 e^-, respectively, in the two sites. These were accounted for by 0.096 Cs atoms and 0.16 H_2O molecules (per 18 O atoms).

The final $R_{(unweighted)}$ value was 0.023 for 32 parameters and 393 observations {$R_{(weighted)} = 0.024$, weights $w = 1/[\sigma^2(F_{obs}) + 0.0003F^2_{obs}]$}. The atomic scattering curves of neutral Si, O, Be, Al, Cs were taken from volume IV of the *International Tables for X-ray Crystallography* (Ibers and Hamilton, 1974).

Sample no. 2. A fragment of aquamarine with dimensions 0.15 × 0.12 × 0.10 mm was selected for the X-ray work on the diffractometer. The lattice dimensions, measured as for sample no. 1, are $a = 9.218(2)$ and $c = 9.197(2)$ Å; c/a is 0.998, showing a limited amount of octahedral substitution. The intensity data were measured and treated with the same procedure described for sample no. 1: at the end of the refinement a residual electron density maximum was observed on the difference Fourier map at site 2a, corresponding to 3.85 e^-. By ascribing this density to an O atom, this value would correspond to 0.48 H_2O molecules pfu. The same density in 2a could be ascribed to 0.35 Na atoms without significant change in the agreement factor. On the basis of the X-ray refinement, the actual situation is such that the Na atoms and the H_2O molecules detected by chemical analysis and IR spectroscopy are in site 2a. The final R value is 0.022 for 29 parameters and 415 observed reflections {$R_w = 0.022$, $w = 1/[\sigma^2(F_{obs}) + 0.0015F^2_{obs}]$}.

Observed and calculated structure factors and temperature factors for both samples are listed in Table 2.[1]

Neutron refinement

Single-crystal neutron diffraction data were obtained at the Neutron Research Laboratory, Studsvik, Sweden, using a four-circle Huber diffractometer. The wavelength, 1.207(1) Å, was obtained with a Cu (220) double-crystal monochromator and calibrated against the two sets of beryl unit cell parameters determined by X-ray diffraction. Data for both crystals were obtained at 295 K and, for sample no. 1, also at 30 K. The low temperature was attained using a CTI Cryogenics two-step closed-cycle He cooler. The unit-cell parameters at 30 K were refined from 30 well-determined 2θ values. Measured absorption factors were found to be in close agreement with the values computed from the chemical compositions. An analytical absorption correction was made possible by the preparation of the two crystals as prisms with accurately measured dimensions that gave volumes of 11.5 and 12.4 mm^3, respectively.

The structure refinements were carried out using the crystallographic computing package UPALS (Lundgren, 1982), and in the final stages included anisotropic displacement parameters for all framework atoms, isotropic displacement parameters for extraframework cations, O and H atoms of H_2O, and freely refined occupancy parameters for channel species and scattering lengths for Al octahedral and Be tetrahedral sites. Neutron scattering lengths for all atoms are from Koester et al. (1981). An extinction correction was applied using an isotropic model for a type I crystal; both a Gaussian and a Lorentzian distribution of mosaic blocks were compared, and the latter was found to provide a more satisfactory fit for the high-intensity, low-angle reflections. Final agreement factors are as follows: sample no. 1 at 295 K, $R_{(unweighted)} = 0.034$, at 30 K, $R_{(unweighted)} = 0.052$; sample no. 2, at 295 K, $R_{(unweighted)} = 0.033$. Refined parameters, temperature factors, and observed and calculated structure factors for all three neutron data structure refinements are given in Table 2[1]. Details of data measurement and refinement parameters are summarized in Table 3.

Table 3. Neutron data measurement, reduction, and refinement parameters for beryl

	No. 1, morganite	No. 1, morganite	No. 2, aquamarine
T (K)	295(1)	30(2)	295(1)
a (Å)	9.208(2)	9.197(9)	9.218(2)
c (Å)	9.197(2)	9.202(8)	9.197(2)
μ (cm^{-1})	0.42	0.42	0.04
Transm. factor range	0.917–0.931	0.917–0.931	0.991–0.993
Max. (sin θ)/λ	0.662	0.662	0.660
No. of unique refl. collected	300	304	299
No. refl. in final cycles	300	302	265
No. of parameters refined	38	42	39
$R(F)$	0.031	0.051	0.027
$R(F^2)$	0.041	0.057	0.032
$R_w(F^2)$	0.057	0.057	0.042
S	1.0435	1.0762	1.0682
$c1$*	0.040	0.020	0.025
$c2$*	0.020	0.800	0.010

* L.S. weights: $w = [\sigma^2(F_o^2) + (c1 \cdot F_o^2)^2 + c2]^{-1}$.

The results are in good general agreement with the X-ray single-crystal refinements and with the results of the chemical analyses. Some discrepancies in atomic coordinates, markedly for sample no. 1, may be ascribed to physical differences in techniques and crystals utilized in the refinements. Furthermore, an overcompensation of the negative density regions in the channels resulting from the inability of the model to take full account of the disordered H atoms would have the effect of shifting the refined O1 position closer to the channel center, which in turn would affect Si and O2 positions of the neutron data refinements. Owing to neutron scattering length differences, population refinements were successfully carried out for Li substitution for $^{[4]}$Be in crystal no. 1 and for Fe substitution for $^{[6]}$Al in crystal no. 2. A cation distribution model that assumes the Cs content from EPMA to be located in site 2a gave the best results in terms of its atomic displacement parameter and allowed refinement

[1] For a copy of Table 2, order Document AM-93-528 from the Business Office, Mineralogical Society of America, 1130 Seventeenth Street NW, Suite 330, Washington, DC 20036, U.S.A. Please remit $5.00 in advance for the microfiche.

Table 4. Final atomic coordinates, atomic displacement parameters (Å²), and occupancy factors for beryl samples 1 and 2

		x	y	z	B*	G
			Sample no. 1			
Si	(A)	0.3895(4)	0.1182(4)	0	0.34(7)	1.0
	(B)	0.3889(2)	0.1182(1)	0	0.29(4)	1.0
	(C)	0.3880(1)	0.1165(1)	0	0.32(2)	1.0
Be	(A)	½	0	¼	0.33(7)	0.993(14)**
	(B)	½	0	¼	0.46(3)	1.000(6)**
	(C)	½	0	¼	0.60(4)	1.0
Al	(A)	⅔	⅓	¼	0.26(9)	1.0
	(B)	⅔	⅓	¼	0.33(5)	1.0
	(C)	⅔	⅓	¼	0.35(2)	1.0
O1	(A)	0.3065(3)	0.2357(3)	0	0.65(6)	1.0
	(B)	0.3062(1)	0.2351(1)	0	0.85(3)	1.0
	(C)	0.3092(2)	0.2364(2)	0	0.87(5)	1.0
O2	(A)	0.4988(2)	0.1468(2)	0.1449(2)	0.62(4)	1.0
	(B)	0.49842(8)	0.14681(9)	0.14499(9)	0.71(3)	1.0
	(C)	0.4988(1)	0.1459(1)	0.1454(1)	0.62(3)	1.0
Ow	(A)	0	0	¼	2.0(2)	0.72(4)
	(B)	0	0	¼	3.6(2)	0.61(3)
Cs	(A)	0	0	¼	2.0(2)	0.083†
	(B)	0	0	¼	3.6(2)	0.083†
	(C)	0	0	¼	7.8(5)	0.096(3)
Na	(A)	0	0	0	1.5(6)	0.24(3)
	(B)	0	0	0	2.1(6)	0.24(3)
Ow	(C)	0	0	0	4.9(6)	0.16(1)
H	(A)	0.092(7)	0.062(7)	0.316(4)	5.0	0.123(7)
	(B)	0.072(5)	0.090(4)	0.318(3)	4.0	0.105(5)
			Sample no. 2			
Si	(B)	0.3872(1)	0.1157(1)	0	0.23(4)	1.0
	(C)	0.38735(4)	0.11563(4)	0	0.24(2)	1.0
Be	(B)	½	0	¼	0.45(3)	1.0
	(C)	½	0	¼	0.45(2)	1.0
Al	(B)	⅔	⅓	¼	0.27(7)	1.007(21)‡
	(C)	⅔	⅓	¼	0.21(2)	1.0
O1	(B)	0.3098(1)	0.2363(1)	0	0.69(4)	1.0
	(C)	0.3099(1)	0.2365(1)	0	0.80(3)	1.0
O2	(B)	0.49866(8)	0.14541(8)	0.14517(8)	0.46(3)	1.0
	(C)	0.4986(1)	0.1454(1)	0.1452(1)	0.47(2)	1.0
Na	(B)	0	0	¼	5.0(9)	0.016†
Ow	(B)	0	0	¼	5.0(9)	0.24(2)
	(C)	0	0	¼	8.5(6)	0.48(4)
H	(B)	0	0	0.165(10)	4.0	0.13(4)

Note: Cell contents (Z = 2) = G·number of equipoints. (A) refers to neutron refinement at 30 K. (B) refers to neutron refinement at 295 K. (C) refers to X-ray refinement.

* B is B_{eq} for framework atoms and B_{iso} for cations and H_2O molecules in the channel.

** Refined as 0.894 Be + 0.106 Li.

† Fixed at EPMA values.

‡ Refined as 0.985 Al + 0.015 Fe.

Table 5. Relevant bond distances (Å) and angles (°) from X-ray and neutron refinements

	Neutron refinement (30 K)	Neutron refinement (295 K)	X-ray refinement
		Sample no. 1	
Si-O1	1.601(4)	1.600(2)	1.596(1)
Si-O1	1.604(4)	1.604(2)	1.598(1)
Si-O2 × 2	1.610(2)	1.612(1)	1.620(2)
Mean	1.606	1.607	1.609
Be-O2 × 4	1.666(2)	1.6673(8)	1.657(1)
Al-O2 × 6	1.901(2)	1.9031(8)	1.905(1)
Ow-H × 12	0.97(5)	0.98(3)	—
H-Ow-H	101.8(5.3)	100.7(3.5)	
	110.1(6.4)	108.7(4.7)	
	116.9(6.6)	119.6(4.0)	
		Sample no. 2	
Si-O1		1.593(2)	1.596(1)
Si-O1		1.597(2)	1.596(1)
Si-O2 × 2		1.622(1)	1.622(1)
Mean		1.609	1.609
Be-O2 × 4		1.6562(7)	1.655(1)
Al-O2 × 6		1.9094(7)	1.909(1)
Ow-H × 2		0.78(10)	—

of the Na occupancy in site 2b very close to the value obtained by EPMA for crystal no. 1.

The equivalent displacement parameters at 30 K are generally smaller (10–30%) than those at 295 K, as expected for silicate minerals, except for the Si atom, owing to a high correlation of its displacement parameter with the extinction coefficient during the refinement.

Difference Fourier maps obtained from the low-temperature data set obtained from the same crystal allowed allocation of H_2O molecules to site 2a based on the presence of H atoms adjacent to this position above and below the mirror plane, in a statistical arrangement around the sixfold axis and at a distance of 0.98(3) Å from the O at 0,0,¼. In crystal no. 2 the scattering power in site 2a, refined as Na, gave an occupancy in great excess of the EPMA results. The final refinement was carried out with the Na amount at 0,0,¼ fixed at the EPMA value (0.016 atoms pfu), and the residual site scattering was refined as an O atom in H_2O. The assignment of H_2O to site 2a is confirmed by negative regions above and below the mirror plane, located on the sixfold axis, which are interpreted as positions occupied by the H atoms of H_2O. For all H atoms, because of the high correlation between occupancy and atomic displacement parameters, the latter were fixed in the last cycles at average values obtained by alternate refinements of the two variables.

Atomic positional and displacement parameters and relevant bond distances are compared with those from X-ray refinements in Tables 4 and 5, respectively.

Results and discussion

Sample no. 1

The neutron data structure refinements at room and low temperature lead to the following interpretation of the occupancy pattern within the channels.

Na occupies the smaller 2b site at 0,0,0; Cs occupies the larger 2a site at 0,0,¼ and, when this occurs, the nearest 2b site is empty. The 2a site is also occupied by H_2O molecules with their H atoms distributed on 12 equipoints in a disordered fashion and directed away from the Na atoms. Figure 3 clearly shows the H sites in the difference Fourier map obtained from the 30-K data set. The O atoms in H_2O are at 2.3 Å from Na. The H_2O environmental constraints in this alkali-rich sample are compatible with two possible arrangements of the H_2O molecules; one having both H atoms on the same **ab** plane, the other with one H atom above and one below the O atom in site 2a, although two mirror-related H atoms cannot be present simultaneously because of geometric constraints. The in-plane interpretation is consistent with

the spectroscopic studies showing the H-H vector of the H_2O monomer to be perpendicular to the c axis in the presence of Na atoms in the channels (type II H_2O: Wood and Nassau, 1967, 1968; Aines and Rossman, 1984).

As regards the tetrahedral substitution, the negative scattering length contributed by Li in the Be site yielded a population refinement corresponding to 2.68 Be and 0.32 Li atoms pfu.

The X-ray refinement has clearly left some uncertainties as to the distribution of Na and H_2O molecules in the channel sites and could not shed any light on the tetrahedral Be-Li substitution.

Sample no. 2

The neutron data structure refinement shows that the small amounts of Na and H_2O are actually located at site 2a. All attempts at refining the O atoms of H_2O at 0,0,0 were unsuccessful. As to the geometry of the H atoms, their arrangement seems to follow a completely different pattern with respect to that found in sample no. 1. The negative peak located on the sixfold axis at 0.78 Å from the 0,0,¼ site is interpreted as a proton position of the H_2O molecule. One possible interpretation of the H_2O molecule orientation calls for one of the protons to be essentially ordered in this position on the symmetry axis, whereas the other proton and the O atom of H_2O would be disordered on several off-axis positions around site 2a. This model assumes a normal geometry of the H_2O molecule, having the H-H vector inclined at about 38° to the c axis, and would explain the otherwise unreasonably short O-H distance. In this interpretation, the two H atoms would belong to different H_2O molecules with statistical occupancy of the two mirror-related positions. Another possible interpretation may however be inferred, with the two H atoms above and below site 2a belonging to the same H_2O molecule, with its H-H vector parallel to the c axis and having the O atom disordered on the mirror plane. The latter geometry is consistent with a normal H-H distance of 1.56 Å in a nonbonded H_2O molecule, with a type I H_2O orientation as found by IR spectroscopy in alkali-poor beryl (Wickersheim and Buchanan, 1959, 1965; Wood and Nassau, 1967, 1968), and with a free rotation of type I H_2O around the sixfold axis (Rehm, 1974).

Scattering lengths refinement for Al and Fe in the octahedral site yielded 1.97 Al and 0.03 Fe atoms pfu compared with 1.94 Al and 0.06 Fe, respectively, from EPMA data (see Table 1). Given the small amount of Na present in the structure, virtually all Fe must be in the trivalent state.

Conclusions

The substitutional pattern within the beryl framework is confirmed (Aurisicchio et al., 1988) by both X-ray and neutron refinements. As to the distribution of H_2O molecules and alkalis in the channels, the structure refinements based on both neutron and X-ray scattering data confirm that Cs is invariably located at 0,0,¼ (the larger 2a site). Neutron data also clearly indicate that Na is located at 0,0,0 (the smaller 2b site) when H_2O molecules are present in site 2a (sample no. 1), whereas in slightly hydrated beryl (sample no. 2), they give an indication that Na ions and H_2O molecules occupy site 2a. These results favor the hypothesis that H_2O molecules, anchored by H bonds to the 2a site, would act as upper and lower support of the Na atoms located at the center of the six-membered rings of Si tetrahedra at 0,0,0 (site 2b). The implication is that the H_2O molecules form $Na(H_2O)_2$ solvated species with the Na ions in the beryl channels, in agreement with crystal-chemical studies on alkali-rich hydrous beryl showing H_2O to Na ratios in excess of 2:1 (Hawthorne and Černý, 1977; Sanders and Doff, 1991). When little or no H_2O is present, the Na cations and the few H_2O molecules prefer the larger 2a sites between the six-membered rings of Si tetrahedra.

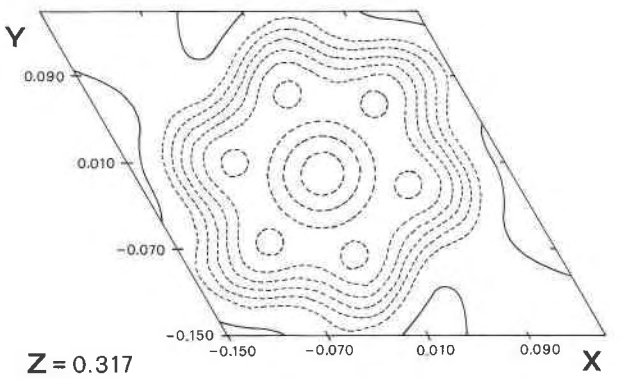

Fig. 3. Difference Fourier map at $z = 0.317$ from 30-K neutron data on sample no. 1, showing the strongly negative regions due to the presence of H atoms around the 2a position at 0,0,¼. Contours at arbitrary intervals.

Neutron diffraction site population analysis confirmed the general substitutional pattern, if one assumes framework charge compensation in beryl by means of ionic species in the structural channels and involving alkali atoms hydration. There is either a weak or no H bonding interaction between the statistically distributed H_2O molecules and the framework O atoms, and the observed geometry of the H_2O monomers is consistent with the orientations of the molecular dipoles as observed by polarized IR spectroscopy.

Acknowledgments

R. Tellgren and H. Rundlof of the Studsvik Neutron Research Laboratory are acknowledged for data measurement, P. Černý for providing the pollucite EPMA standard, and G. Molin for the Cameca probe analysis. The Italian C.N.R. is acknowledged for financing the EPMA laboratory at Modena University and for an Advanced Crystallography grant to R.R. The Italian M.U.R.S.T. provided general financial support (40% of funds). K.S. thanks the Swedish Natural Science Research Council for financial support.

References cited

Aines, R.D., and Rossman, G.R. (1984) The high temperature behaviour of water and carbon dioxide in cordierite and beryl. American Mineralogist, 69, 319–327.

Albee, A.L., and Ray, L. (1970) Correction factors for electron-probe microanalysis of silicates, oxides, carbonates, phosphates and sulphates. Analytical Chemistry, 42, 1408–1414.

Aurisicchio, C., Fioravanti, G., Grubessi, O., and Zanazzi, P.F. (1988) Reappraisal of the crystal chemistry of beryl. American Mineralogist, 73, 826–837.

Brown, G.E., Jr., and Mills, B.A. (1986) High-temperature structure and crystal chemistry of hydrous alkali-rich beryl from the Harding pegmatite, Taos County, New Mexico. American Mineralogist, 71, 547–556.

Černý, P. (1975) Alkali variations in pegmatitic beryl and their petrogenetic implications. Neues Jahrbuch für Mineralogie Abhandlungen, 123, 198–212.

Černý, P., and Simpson, F.M. (1977) The Tanco pegmatite at Bernik Lake, Manitoba. IX. Beryl. Canadian Mineralogist, 15, 489–499.

Gibbs, G.V., Breck, D.W., and Meagher, E.P. (1968) Structural refinements of hydrous and anhydrous synthetic beryl, $Al_2(Be_3Si_6)O_{18}$, and emerald, $Al_{1.9}Cr_{0.1}(Be_3Si_6)O_{18}$. Lithos, 1, 275–285.

Hawthorne, F.C., and Černý, P. (1977) The alkali-metal positions in Cs-Li beryl. Canadian Mineralogist, 15, 414–421.

Ibers, J.A., and Hamilton, W.C., Eds. (1974) International tables for X-ray crystallography, vol. IV, 366 p. Kynoch, Birmingham, U.K.

Koester, L., Rauch, H., Herkens, M., and Schroeder, K. (1981) Summary of neutron scattering lengths. Kernforschungsanlage Report Jül-1755.

Lundgren, J.O. (1982) Uppsala crystallographic computer programs. University of Uppsala, Sweden, Report no. UUIC-B13-4-05.

North, A.C.T., Phillips, D.C., and Mathews, F.S. (1968) A semi-empirical method of absorption correction. Acta Crystallographica, A24, 351–359.

Pouchou, J.-L., and Pichoir, F. (1988) A simplified version of the "PAP" model for matrix correction in EPMA. In D.E. Newbury, Ed., Microbeam analysis 1988, p. 315–318. San Francisco Press, San Francisco, California.

Rehm, H.J. (1974) Paraelektrische resonanz und dielektrische Dispersion von Wasser in Beryll-Einkristallen. Zeitschrift für Naturforschung, 29A, 1558–1571.

Sanders, I.S., and Doff, D.H. (1991) A blue sodic beryl from southeast Ireland. Mineralogical Magazine, 55, 167–172.

Sheldrick, G.M. (1976) SHELX-76: Program for crystal structure determination. University of Cambridge, Cambridge, England.

Sherriff, B.L., Grundy, D.H., Hartman, J.S., Hawthorne, F.C., and Černý, P. (1991) The incorporation of alkalis in beryl: Multi-nuclear MAS NMR and crystal structure study. Canadian Mineralogist, 29, 271–285.

Vorma, A., Sahama, T.G., and Haapala, I. (1965) Alkali position in the beryl structure. Comptes Rendues de la Société Geologique de Finlande, 37, 119–124.

Wickersheim, K.A., and Buchanan, R.A. (1959) The near infrared spectrum of beryl. American Mineralogist, 44, 440–444.

——— (1965) Some remarks concerning the spectra of water and hydroxyl groups in beryl. Journal of Chemical Physics, 42, 1468–1469.

Wood, D.L., and Nassau, K. (1967) Infrared spectra of foreign molecules in beryl. Journal of Chemical Physics, 47, 2220–2228.

——— (1968) The characterization of beryl and emerald by visible and infrared absorption spectroscopy. American Mineralogist, 53, 777–800.

Manuscript received September 24, 1992
Manuscript accepted March 4, 1993